Convergent evolution and structural adaptation to the deep ocean in the protein folding chaperonin CCTα

Alexandra A.-T. Weber[1,2,3*], Andrew F. Hugall[1], Timothy D. O'Hara[1]

[1]Sciences, Museums Victoria, GPO Box 666, Melbourne VIC 3001, Australia

[2]Centre de Bretagne, REM/EEP, Ifremer, Laboratoire Environnement Profond, 29280 Plouzané, France

[3]Zoological Institute, University of Basel, Vesalgasse 1, 4051 Basel, Switzerland

*Author for Correspondence: Alexandra A.-T. Weber, Sciences, Museums Victoria, GPO Box 666, Melbourne VIC 3001, Australia, +61 3 8341 7641, aweber@museum.vic.gov.au

Abstract

The deep ocean is the largest biome on Earth and yet it is among the least studied environments of our planet. Life at great depths requires several specific adaptations, however their molecular mechanisms remain understudied. We examined patterns of positive selection in 416 genes from four brittle star (Ophiuroidea) families displaying replicated events of deep-sea colonization (288 individuals from 216 species). We found consistent signatures of molecular convergence in functions related to protein biogenesis, including protein folding and translation. Five genes were recurrently positively selected, including CCTα (Chaperonin Containing TCP-1 subunit α), which is essential for protein folding. Molecular convergence was detected at the functional and gene levels but not at the amino-acid level. Pressure-adapted proteins are expected to display higher stability to counteract the effects of denaturation. We thus examined *in silico* local protein stability of CCTα across the ophiuroid tree of life (967 individuals from 725 species) in a phylogenetically-corrected context and found that deep sea-adapted proteins display higher stability within and next to the substrate-binding region, which was confirmed by *in silico* global protein stability analyses. This suggests that CCTα not only displays structural but also functional adaptations to deep water conditions. The CCT complex is involved in the folding of ~10% of newly synthesized proteins and has previously been categorized as 'cold-shock' protein in numerous eukaryotes. We thus propose that adaptation mechanisms to cold and deep-sea environments may be linked and highlight that efficient protein biogenesis, including protein folding and translation, are key metabolic deep-sea adaptations.

Key words

Echinodermata; TCP-1; protein folding; positive selection; protein stability; pressure adaptation

Introduction

The deep ocean (>200m) covers approximately two-thirds of the global sea floor area, yet it is among the least studied environments of our planet in terms of biodiversity, habitats and ecosystem functioning (Ramirez-Llodra et al. 2010). It harbors specific environmental conditions such as high hydrostatic pressure (on average ~400 atm), low temperatures (0-4°C), absence of light and scarcity of food. Life at great depths requires multiple metabolic adaptations resulting in a physiological bottleneck (Gross & Jaenicke 1994) limiting the vertical distribution of species (Brown & Thatje 2014; Somero 1992). It has also been proposed that high pressure may drive speciation events (Brown & Thatje 2014; Gaither et al. 2016). Numerous cellular processes such as enzymatic processes, protein folding, assembly of multi-subunit proteins and lipoprotein membranes are impacted by high pressure and low temperature (Carney 2005; Jaenicke 1991; Pradillon & Gaill 2007; Somero 1992). More specifically, cellular mechanisms of deep-sea adaptation have been recently reviewed (Yancey 2020) and include changes in membrane fluidity (high pressure and low temperature rigidify membranes), extrinsic adaptations (i.e. changes in the cellular milieu such as the expression of molecular chaperones or increased concentration of piezolytes, i.e. stabilizing solutes), and intrinsic adaptations (i.e. changes in protein sequences). An essential intrinsic adaptation of deep-sea proteins is their increased stability (i.e. more resistant to denaturation) compared to their shallow-water counterparts (Gross & Jaenicke 1994; Siebenaller 2010; Somero 1992, 1990, 2003). This has been shown in numerous studies, which mainly focused on a handful of proteins (such as lactate dehydrogenase) in deep-sea fishes (Dahlhoff & Somero 1991; Lemaire et al. 2018; Morita 2008, 2003; Siebenaller & Somero 1979, 1978; Suka et al. 2019; Wakai et al. 2014). Interestingly, patterns of protein adaptation to temperature show higher flexibility (i.e. decreased stability) with decreasing temperature (Fields et al. 2015; Saarman et al. 2017). As pressure and temperature strongly co-vary in the deep sea - temperature decreases as pressure increases - it therefore can be difficult to disentangle the respective combined or opposing effects of these factors on protein stability evolution.

Patterns of positive selection have been investigated to uncover genes underlying adaptation to specific environments, including the deep-sea, in non-model species (Kober & Pogson 2017; Lan et al. 2018; Oliver et al. 2010; Sun et al. 2017; Zhang et al. 2017; Weber et al. 2017). Although valuable, these studies typically focus on a single or few shallow-deep transitions in a limited number of species, and thus lack the comparative power to separate confounding effects. With almost 2100 species, brittle stars (Ophiuroidea) are a large and ancient class of echinoderms (Stöhr et al. 2017, 2012). These diverse marine invertebrates have colonized every marine habitat, highlighting their strong adaptive abilities. Furthermore, their phylogeny is well-resolved (O'Hara et al. 2017, 2014) and they represent a major component of the deep-sea fauna in terms of abundance and species diversity (Christodoulou et al. 2019a; Christodoulou et al. 2019b), making them important models for marine biodiversity and biogeography (O'Hara et al. 2019; Woolley et al. 2016). It is usually assumed that deep-sea organisms colonized the deep-sea from shallow waters (Brown & Thatje 2014); however, colonization from deep to shallow waters has also been reported (Bribiesca-Contreras et al. 2017; Brown & Thatje 2014). Four large independent ophiuroid families (Amphiuridae, Ophiodermatidae, Ophiomyxidae and Ophiotrichidae) have a common ancestor from shallow water with extant species occurring in deep and shallow seas (Bribiesca-Contreras et al. 2017). Due to these repeated and independent deep-sea colonization events, these four brittle star families provide an ideal framework to test for convergent molecular evolution to the deep sea.

Materials and Methods

Phylogenomic data generation and processing

The data used in this study is an extension (436 additional samples) of a previously published exon-capture phylogenomic datamatrix of 1484 exons in 416 genes for 708 individual ophiuroid samples representative of the whole class Ophiuroidea (O'Hara et al. 2019). The full dataset used here encompassed 1144 individual ophiuroid samples accounting for 826 species. Details on specimen collection, environmental parameters and list of species are available in Table S1. The set of 416 single-copy genes were first determined in a phylogenomic analysis to resolve the phylogeny of Ophiuroidea (O'Hara et al. 2014). These genes were rigorously screened to be one-to-one orthologs in 52 ophiuroid transcriptomes (representative of the entire class), in the sea urchin *Stronlgylocentrotus purpuratus*, the hemichordate *Saccoglossus kowalevskii* and the fish *Danio rerio*. The subsequent exon-capture system laboratory, bioinformatic and phylogenetic procedures are described in previous works (O'Hara et al. 2017; Hugall et al. 2016) and summarized in dryad packages https://doi.org/10.5061/dryad.db339/10 and https://datadryad.org/stash/dataset/doi:10.5061/dryad.rb334. Briefly, base-calling used a minimum read coverage of five. Exon boundaries were initially based on the *Strongylocentrotus purpuratus* and *Danio rerio* genomes, and then revised using the exon-capture read mapping information. For all selection analyses, each codon immediately adjacent to exon boundaries was ignored. The primary data had IUPAC-coded heterozygous sites, which were then randomly resolved. However, these sites had little influence as both ambiguity-coded and randomly resolved datasets returned the same positive selection test results. A global phylogenetic tree of all 1144 samples for 416 genes (273kb sites) was generated via RAxML v.8.2.11 (Stamatakis 2014) using a codon position partition model. First a fully-resolved all-compatible consensus topology was generated from 200 RAxML fast bootstrap samples (the -f –d command), onto which branch lengths were then optimized using a codon position GTR-Γ model (the -f –e command). The tree was then rooted according to (O'Hara et al. 2017) defining the sister superorders Ophintegrida and Euryophiurida.

Four brittle star families were investigated that included species displaying independent events of deep-sea colonization from shallow-water (Bribiesca-Contreras et al. 2017): Amphiuridae (111 individuals from 95 species, depth range: -0.5m to -5193m; temperature range: -1.6°C to 28.8°C), Ophiodermatidae (60 individuals from 38 species, depth range: -0.5m to -1668m; temperature range: 2.6°C to 28.3°C), Ophiomyxidae (41 individuals from 29 species, depth range: -1.5m to -792m; temperature range: 4.6°C to 28.7°C) and Ophiotrichidae (78 individuals from 62 species, depth range: -1m to -405m; temperature range: 10.5°C to 29.5°C) (Figure 1A). Positive selection analyses were conducted separately per family. 1664 alignments were generated, representing each gene (416) in each family (4). In each alignment, a maximum of 30% missing data per sequence was allowed. Alignments that lacked deep species (>200m) after filtering were not used. As all these four families belong to the superorder Ophintegrida, sequences of *Asteronyx loveni* belonging to the sister superorder Euryophiurida (Asteronychidae) were used as outgroups. After filtering, 1649 alignments were available for further analyses.

Phylogenetic reconstruction and positive selection analyses

For each of the 1649 alignments, a Maximum-Likelihood phylogeny was reconstructed using RAxML v.8.2.11 with the following parameters: -x 12345 -# 100 -f a -m GTRGAMMA -p 12345

128 (Figure 1B). Deep (>200m) species (tips) and monophyletic groups of deep species (nodes)
129 were labeled as "Foreground" branches for positive selection analyses (Amphiuridae: 46
130 species; 11 independent events of deep-sea colonization; Ophiodermatidae: 7 species; 4
131 independent events; Ophiomyxidae: 10 species; 4 independent events; Ophiotrichidae: 4
132 species; 4 independent events). Then, the package HyPhy was used to conduct several positive
133 selection analyses (Figure 1C): 1) BUSTED (Branch-site Unrestricted Statistical Test for Episodic
134 Diversification) (Murrell et al. 2015) to test for gene-wide positive selection (at least one site on
135 at least one branch); 2) aBSREL (adaptive Branch-Site Random Effects Likelihood) (Smith et al.
136 2015) to detect specific branches evolving under episodic positive selection; 3) MEME (Mixed
137 Effects Model of Evolution) (Murrell et al. 2012) to find sites evolving under episodic positive
138 selection. 4) MNM method; it has been shown recently that mutations at adjacent sites often
139 occur as a result of the same mutational event (i.e. multinucleotide mutations, MNMs) and
140 therefore may bias classical branch-site tests for positive selection (Venkat et al. 2018). The
141 authors of that study developed a new model of positive selection detection incorporating
142 MNMs, which we also used on deep lineages (>200m). For each gene, p-values were corrected
143 for multiple testing using the Holm method (Holm 1979). The p-value significance level used for
144 all the positive selection detection methods was 0.05. Finally, we used: 5) RELAX (Wertheim et
145 al. 2014) to test for relaxation of selection, and exclude potential candidate genes displaying
146 relaxation of selection. For each of the four families, positively selected candidate genes of each
147 method were overlapped on a Venn diagram (Figures 1C and S1). To be considered as a
148 candidate gene for positive selection in one family and to minimize the risk of false positives, a
149 gene had to display a significant signal in at least three out of four methods including MEME and
150 MNM (BUSTED, MEME, MNM or MEME, MNM, aBSREL) and not display relaxation of selection
151 (RELAX). This set of candidates was used for functional annotation. Final sets of positively
152 selected genes per family were then compared among each other to test for convergent
153 evolution. To confirm that positive selection was detected only in deep-sea lineages, positive
154 selection was also tested in shallow-water lineages for the five genes displaying convergent
155 positive selection signatures (CCTα, PFD3, tkt, rpl34, rpl8; see Results, Tables 1, S3). For each
156 family, the same number of shallow-water species as was used for deep-water species was
157 randomly labeled as 'Foreground' in each gene tree and positive selection tests were performed
158 for the five methods as described above.

159 *Gene Ontology annotations and amino-acid convergence analyses*

160 To explore which functions may be involved in deep-sea adaptation, the representative
161 sequence of each of the 416 genes was extracted from the sea urchin *Strongylocentrotus*
162 *purpuratus* genome and blasted against the nr database from NCBI using BLAST+. We used *S.*
163 *purpuratus* as reference because sequence annotation for this species is of high quality (no high-
164 quality brittle star reference genome is currently available) and to use a single complete
165 representative sequence for each gene. The top 50 hits were extracted and loaded in BLAST2GO
166 v.4.1. for annotation (Conesa et al. 2005). Mapping, annotation and slim ontology (i.e. GO
167 subsets of broader categories) were performed with BLAST2GO using default parameters,
168 except for the annotation cut-off parameter, which was set to 45. GO categories were described
169 using the level 3 of slim ontology.

170 CCTα, the only candidate gene displaying positive selection signal in three families (see Results)
171 was further analyzed for signatures of convergent evolution. Specifically, amino-acid profiles
172 were investigated for convergent shifts using PCOC (Rey et al. 2018). This method, which has

173 been shown to display high sensitivity and specificity, detects convergent shifts in amino-acid
174 preferences rather than convergent substitutions. The CCTα amino-acid alignment
175 encompassing the four families and outgroups was used to generate a maximum-likelihood
176 phylogeny as previously described but this time using the PROTGAMMAWAG protein model of
177 sequence evolution (Figure S2). For each family, positively selected branches resulting from
178 aBSREL analyses were labeled as foreground branches (i.e. the branches with the convergent
179 phenotype in the nucleotide topology) in four different scenarios: i) Amphiuridae,
180 Ophiodermatidae, Ophiomyxidae; ii) Amphiuridae, Ophiodermatidae; iii) Amphiuridae,
181 Ophiomyxidae; iv) Ophiodermatidae, Ophiomyxidae. Detection of amino-acid convergence in
182 these four scenarios was then performed using PCOC and a detection threshold of 0.9 (Rey et al.
183 2018).

184 *Protein structure modeling, protein stability profile and overall protein stability*

185 To infer the position of positively selected mutations on CCTα, the corresponding amino-acid
186 sequence of the individual *Amphiura constricta* MVF214041 was used to obtain the secondary
187 and tertiary protein structures of this gene. This shallow-water species was chosen because its
188 CCTα sequence had no missing data. The secondary structure was modeled using InterPro 72.0
189 web browser (https://www.ebi.ac.uk/interpro/). The protein model was generated using the
190 normal mode of the online Phyre^2 server (http://www.sbg.bio.ic.ac.uk/~phyre2/) (Kelley et al.
191 2015). The online server EzMol 1.22 was used for image visualization and production
192 (http://www.sbg.bio.ic.ac.uk/ezmol/) (Reynolds et al. 2018). The online server NetSurfP-2.0
193 (http://www.cbs.dtu.dk/services/NetSurfP/) was used to predict amino-acid surface
194 accessibility and secondary structures.

195 We then examined the protein stability profiles of CCTα across the whole ophiuroid class (967
196 sequences with less than 30% missing sites, representing 725 species) using eScape v2.1 (Gu &
197 Hilser 2009, 2008). This algorithm calculates a per-site estimate of Gibbs free energy of
198 stabilization based on a sliding window of 20 residues. More specifically, it models the
199 contribution of each residue to the stability constant, a metric that represents the equilibrium of
200 the natively folded and the multiple unfolded states of a protein (D'Aquino et al. 1996). Sites
201 adapted to elevated pressure (or high temperature at atmospheric pressure) are expected to
202 display stabilizing mutations (i.e. more negative delta G values), whereas sites adapted to low
203 temperatures at atmospheric pressure are expected to display mutations increasing flexibility
204 (i.e. decreasing stability, thus more positive delta G values) (Fields et al. 2015; Saarman et al.
205 2017). For each site of the apical domain (codons 203-353), we calculated the average delta G
206 value for all 324 shallow-water species (424 individuals) (0-200m) and 401 deep-water species
207 (543 individuals) (>200m) and their respective standard deviation. To test the difference
208 between these average values in a phylogenetic context, we used phylogenetically-corrected
209 ANOVA (R function phylANOVA of the phytools v.0.6-60 R package; 10,000 simulations). To
210 correct for relatedness among species, we used the global RAxML phylogenetic tree pruned to
211 the 967 tips. To investigate regions rather than individual codons, we contrasted shallow vs.
212 deep species along the whole gene, averaging delta G values across 10 residues and performing
213 a phylogenetically-corrected ANOVA as previously described.

214 Finally, we tested how the mutations at the positively selected sites, and the ones with local
215 stability values significantly different between shallow and deep species in the phylogenetically-
216 corrected ANOVA, impacted the global protein stability. For each one of these sites, we
217 identified 'shallow-water' and 'deep-water' mutations, and used the shallow-water Amphiuridae

218 *Amphiura constricta* MVF214041 sequence as template to add these 'shallow-water' and 'deep-
219 water' mutations one at the time. A model structure for each one of these new sequences was
220 generated using the normal mode of the online Phyre[2] server
221 (http://www.sbg.bio.ic.ac.uk/~phyre2/) (Kelley et al. 2015). The global stability of each model
222 structure was then calculated using the 'stability' function of the program FoldX with default
223 values (Schymkowitz et al. 2005). For each site, the ΔΔG value between 'deep-water' (mutant)
224 and 'shallow-water' (wild-type) mutations was calculated, where ΔΔG > 0.5 kcal/mol indicates
225 stabilizing mutations, ΔΔG < -0.5 kcal/mol indicates destabilizing mutation, and -0.5 kcal/mol <
226 ΔΔG < 0.5 kcal/mol indicates neutral mutations (Khatun et al. 2004; Khan & Vihinen 2010).

227 **Results**

228 *Five genes involved in protein biogenesis are recurrently positively selected in deep-sea brittle*
229 *stars*

230 We used 416 single-copy orthologs from 216 species (288 individuals) of four brittle star
231 families (Figure 1A) to examine patterns of positive selection in deep-sea species (>200m). For
232 each gene of each family, we used four different positive selection methods and one method
233 detecting relaxation of selection (Figure 1B-C). Given that our dataset is not representative of
234 the whole genome, we chose a stringent approach to focus on a few candidate genes displaying
235 strong signals of positive selection. Therefore, we only kept candidate genes that had significant
236 signature of positive selection in at least three methods and which also did not show relaxation
237 of selection. We found 36 candidate genes in Amphiuridae, 9 in Ophiodermatidae, 6 in
238 Ophiomyxidae and none in Ophiotrichidae (Table S2; Figure S1). Four genes involved in embryo
239 development were positively selected in Amphiuridae. Common functions among candidate
240 genes from different families include protein folding, translation (i.e. ribosomal proteins),
241 catabolic process and cell proliferation (Table S2).

242 Five genes were positively selected in at least two families, which are notably involved in
243 protein folding and in translation (Table 1). Among these, CCTα was positively selected in all
244 three families and significant in each one of the selection detection methods (Table 1). To
245 confirm that positive selection was detected only in shallow-deep transition, we performed
246 positive selection analyses on these five common candidate genes but this time labelling
247 shallow-water lineages as 'Foreground'. Most of the genes did not display signatures of positive
248 selection in shallow-water environments, except PFD3 in Amphiuridae and tkt in
249 Ophiotrichidae, which were significant in the BUSTED, aBSREL and MEME methods (Table S3).
250 This suggests that these two genes are evolving faster not only in response to deep-sea
251 conditions but also possibly in response to additional environmental conditions.

Table 1: common positively selected candidate genes in three families and their characteristics (3 of 4 methods, not displaying relaxation of selection). *Positively selected in 4 of 4 methods, not displaying relaxation of selection. italic: common Biological Process annotation.

Gene name	Description	Blast Reference sequence	GO terms: Biological Process	Positively selected in
CCTα *	chaperonin containing TCP1 complex subunit α	XP_780270.1	*protein folding*	Amphiuridae, Ophiodermatidae, Ophiomyxidae
PFD3	prefoldin subunit 3	XP_797937.1	macromolecular complex assembly; protein complex assembly; *protein folding*	Amphiuridae, Ophiodermatidae
tkt*	transketolase 2 isoform X2	NP_1229589.1	biological process	Amphiuridae, Ophiodermatidae
rpl34	subunit ribosomal	XP_797232.1	ribosome biogenesis; *translation*	Amphiuridae, Ophiomyxidae
rpl8	60S ribosomal L8	XP_796001.1	*Translation*	Amphiuridae, Ophiomyxidae

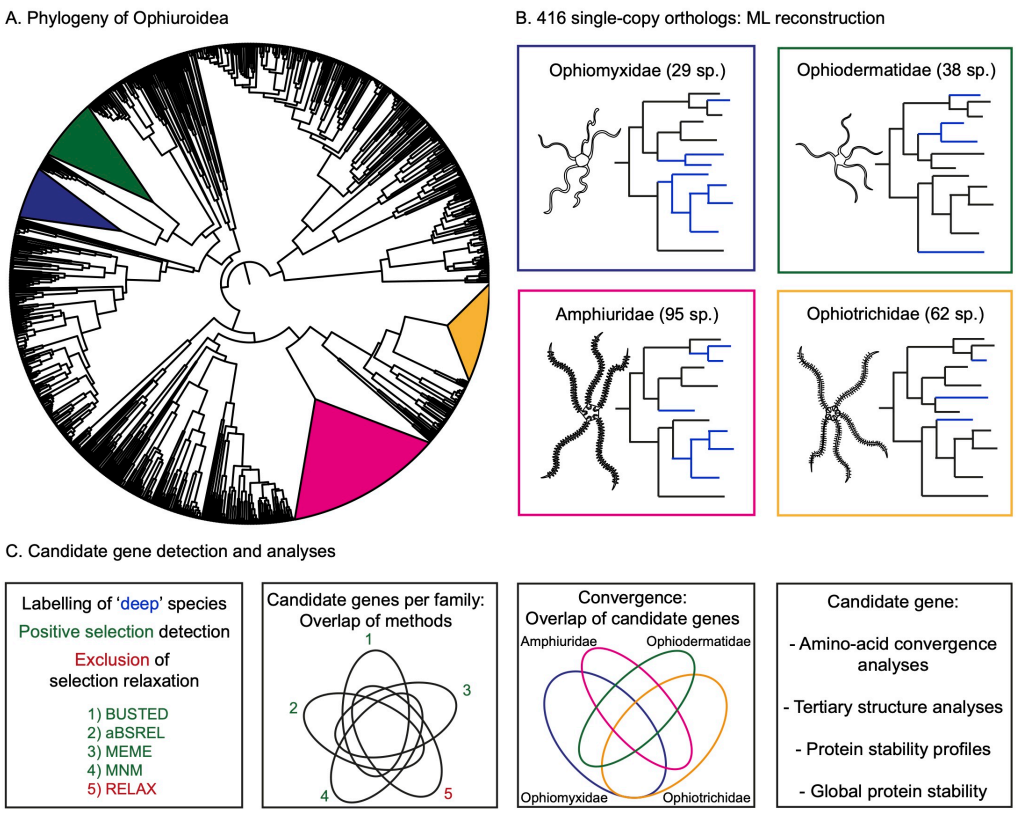

Fig. 1: Workflow used in this study. A: Schematic representation of the phylogeny of Ophiuroidea (redrawn from Christodoulou et al. (2019b)). Four families (288 individuals from 216 species) with a shallow-water common ancestor and extant species in shallow (0-200m) and deep (>200m) environments are highlighted in different colors. The width of each triangle is proportional to the sampled number of species in each family. Ophiomyxidae (blue), Ophiodermatidae (green), Amphiuridae (pink) and Ophiotrichidae (yellow). B: For each family (number of species used in brackets) and each one of the 416 single-copy orthologs, Maximum Likelihood (ML) reconstructions were performed. Trees are drawn for illustration only with the branches of shallow-water (0-200m) species colored in black and deep-water (>200m) species in blue. C: For each resulting ML tree, deep species were labeled as foreground branches and four positive selection detection methods were used (BUSTED, aBSREL, MEME, MNM). To detect and exclude candidate genes displaying relaxation of selection, i.e. accumulation of substitutions not due to increased selection pressure, the method RELAX was used. The final set of candidate genes for each family encompassed genes positively selected in at least 3 methods and not displaying relaxation of selection. Convergent evolution was examined by overlapping candidate genes per family. For the most interesting candidate gene, amino-acid convergence and tertiary structure analyses were performed, and protein stability profiles and global protein stability were calculated.

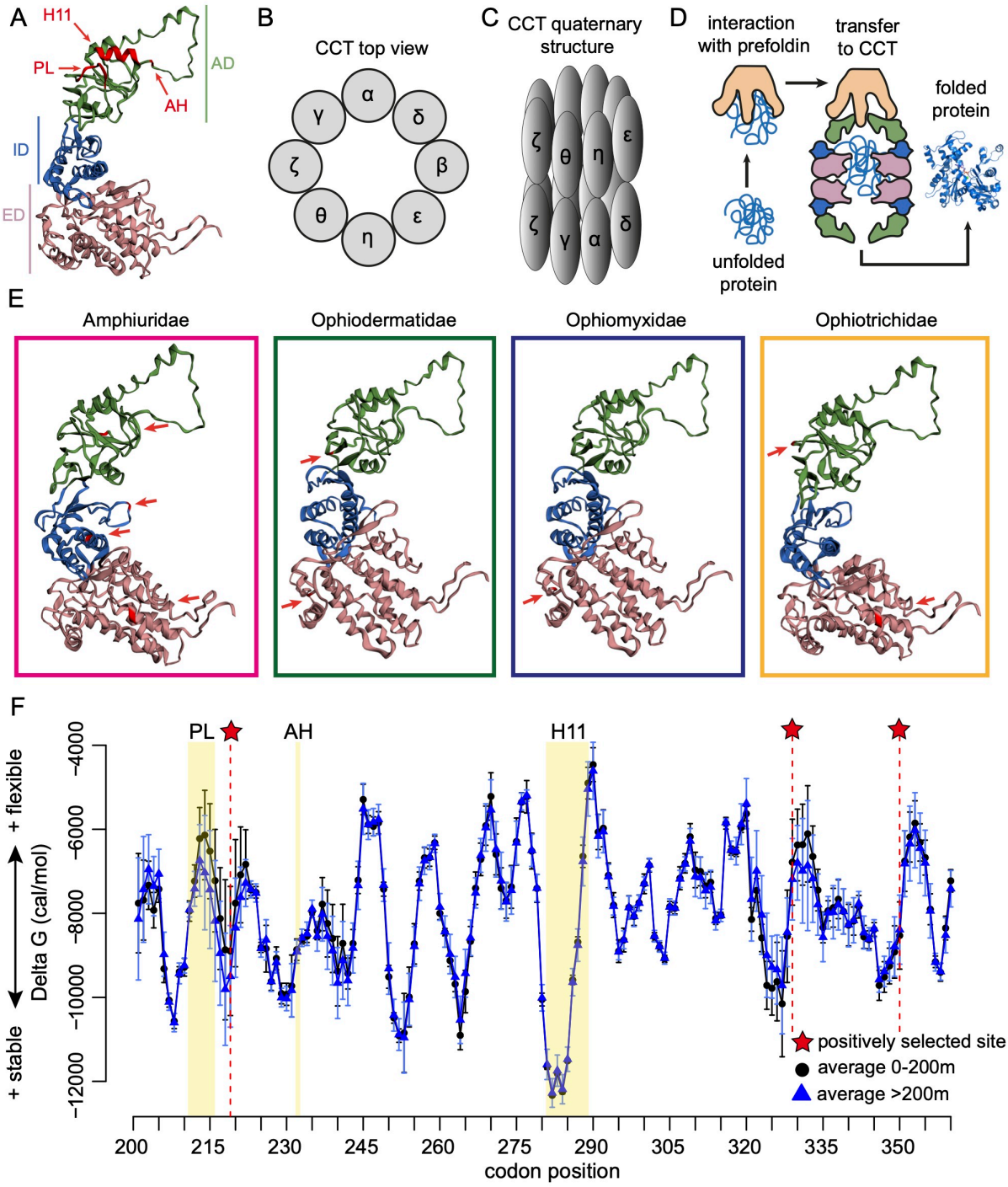

Fig. 2: Structure and function of the CCT complex, selection analyses on CCTα and comparison of local stability values from CCTα apical domain between shallow and deep species. A: Model of tertiary structure of the CCTα subunit. Each subunit is composed of an apical domain (AD; green) containing the substrate binding regions (PL: Proximal Loop; AH: Apical Hinge; H11: Helix 11), an intermediate domain (ID; blue) and an equatorial domain (ED; pink) containing the ATP binding sites and where hydrolysis takes place. B: Model of the top view of the CCT complex, encompassing 8 paralogous subunits. C: Quaternary structure model of the CCT complex encompassing a double ring of 8 paralogous subunits. D: Simplified model of Prefoldin (PFD)-CCT interaction in the folding of newly synthesized actin or tubulin. A-D: Adapted from Bueno-Carrasco & Cuellar, 2018, "Mechanism and Function of the Eukaryotic Chaperonin CCT". E: Localization of the positively selected sites on the tertiary structure of CCTα in the four ophiuroid families investigated. F: Average protein stability profiles and respective standard

deviations (vertical bars) for each codon of the CCTα apical domain in 324 species (424 individuals) from shallow water (0-200m; in black) and 401 species (543 individuals) from deep water (>200m; in blue) representative of the whole ophiuroid class. A smaller (i.e. more negative) value of delta G is indicative of substitutions increasing stability. The substrate binding regions PL, AH and H11 are highlighted as well as the positively selected sites.

CCTα, the sole candidate gene detected as significantly positively selected in three families in the shallow-deep contrast, did not display signatures of positive selection in shallow-water environments (Table S3). It is a subunit of the octameric Chaperonin Containing TCP1 (CCT) complex, a cytosolic eukaryotic chaperonin having a central role in protein folding (Figure 2A-D) (Bueno-Carrasco & Cuéllar 2019; Valpuesta et al. 2005). The three other CCT subunits present in our dataset, CCTδ, CCTε and CCTη, did not display consistent signatures of positive selection; rather, while positive selection was detected at the site level in all subunits, relaxation of selection was detected in all 3 subunits in Amphiuridae (Table S6), indicating that the accumulation of mutations in these subunits is not clearly due to natural selection. Therefore, CCTα was the only one out of four subunits to show consistent signatures of positive selection across methods. The remaining four subunits of the CCT complex could not be tested as they were not present in our dataset.

Interestingly, PFD3, a subunit of the hexameric co-chaperone prefoldin interacting with CCT (Gestaut et al. 2019; Martín-Benito et al. 2002) was positively selected in two families (Amphiuridae: MNM, MEME, BUSTED; Ophiodermatidae: MNM, aBSREL, MEME, BUSTED) (Table 1; Tables S2, S6; Figure 2D), although it was also positively selected in shallow-water Amphiuridae (Table S3). The two other prefoldin subunits present in our dataset (PFD1 and PFD5) did not show a consistent signature of positive selection (Table S4), suggesting that sub-units of this co-chaperone can evolve relatively independently from each other. Finally, two ribosomal proteins (Rpl8 and Rpl34) were recurrently positively selected in Amphiuridae and Ophiomyxidae, while the ribosomal protein S6 was positively selected in Ophiodermatidae (Table 1; Table S2).

CCTα and deep-sea adaptation: convergence at the gene but not amino-acid level

While positive selection was detected at the gene level in three families, positive selection at the site level (MEME) was detected in all four families. The sites displaying positive selection in CCTα were not the same among the four families, except for site 26, which was shared between Amphiuridae and Ophiotrichidae (Figure 2E; Table 2; Table S5). Three sites were found in the equatorial domain, i.e. the ATP binding region, two sites were found in the intermediate domain and three sites were found in the apical domain, i.e. the substrate binding region (Figure 3) (Bueno-Carrasco & Cuéllar 2019). Furthermore, we found that 7 out 8 positively selected sites increased the global protein stability, suggesting that these sites may be involved in structural adaptation of CCTα (Table 2). This is corroborated by the fact that 6 out 8 mutations involve changes towards hydrophobic amino-acids, which are known to increase protein stability (Kellis et al. 1988; Pace et al. 2011). Finally, convergent evolution at the site level was not detected when examining amino-acid profiles (PCOC posterior probabilities at all sites < 0.9).

335 **Table 2:** Summary of the positively selected sites in each family and sites with local stability values
336 significantly different between shallow and deep species. For each site, the 'deep' and 'shallow' amino-
337 acids are reported, as well as their impact on global protein stability: ΔΔG>0.5 kcal/mol: mutations
338 increasing stability; ΔΔG<-0.5 kcal/mol: mutations decreasing stability; -0.5 kcal/mol <ΔΔG<0.5 kcal/mol:
339 neutral mutations in terms of stability. ED: equatorial domain; ID: intermediate domain; AD: apical
340 domain; PS: positively selected. *: the most common amino-acids between shallow and deep species are
341 reported.

Site	Tertiary structure	Detection method	Amino-acid 'deep'	Amino-acid property	Amino-acid 'shallow'	Amino-acid property	ΔΔG [kcal/mol]
26	ED	PS Amphiuridae & PS Ophiotrichidae	A	hydrophobic	S	Polar uncharged	34.7
175	ID	PS Amphiuridae	Y	hydrophobic	S	Polar uncharged	11.8
203*	AD	phylANOVA	P	special case	Q	Polar uncharged	-17.3
215*	AD	phylANOVA	V	hydrophobic	P	special case	2.1
219	AD	PS Ophiotrichidae	I	hydrophobic	T	Polar uncharged	3.7
263*	AD	phylANOVA	H	Positively charged	Q	Polar uncharged	22.9
327*	AD	phylANOVA	S, V	Polar uncharged, hydrophobic	A	hydrophobic	11.9, 30.1
328*	AD	phylANOVA	T	Polar uncharged	S	Polar uncharged	27.6
329	AD	PS Amphiuridae	V	hydrophobic	M	hydrophobic	15.7
350	AD	PS Ophiodermatidae	I	hydrophobic	K	Positively charged	15.7
375	ID	PS Amphiuridae	V	hydrophobic	I	hydrophobic	12.3
462	ED	PS Ophiomyxidae	C	special case	A	hydrophobic	-3.8
465	ED	PS Ophiodermatidae	F	hydrophobic	K	Positively charged	22.9

342

343 *Energetic landscapes reveal structural adaptation within and next to the substrate binding region*

344 Next we calculated site-specific protein stability profiles of CCTα in 967 individuals of 725
345 species representative of the whole Ophiuroidea class, to test the hypothesis that deep-sea
346 adapted proteins are more stable than their shallow-water counterparts. For each site, we
347 compared the average stability measure of 324 shallow-water species (0-200m depth) vs. 401
348 deep-water species (>200m depth), where lower ΔG values correspond to higher stability
349 (Figures 2F, S3A). We focused on the apical domain as it encompasses the substrate binding
350 region, whose position and structure are highly conserved across eukaryotes (Joachimiak et al.
351 2014). This region is composed of the proximal loop (PL), the apical hinge (AH) and Helix 11
352 (H11) (Figures 2A, 3). While AH and H11 are almost invariant across all ophiuroids, the stability
353 measure was lower (i.e. more stable) in deep compared to shallow species within the PL and in
354 two sites following the PL (codons 214-217), close to a positively selected site (codon 219)
355 (Figures 2F, S3A). In contrast, three codons displayed significantly higher flexibility in deep

compared to shallow species (Figure S3A,B), suggesting that increased flexibility may play a role in deep-sea adaptation outside the ligand binding region, possibly related to low temperature. Nevertheless, when averaging ΔG values across 10 codons, only the signal close to PL remained significant in the phylogenetically-corrected ANOVA contrasting stability values of shallow and deep species (Figure S4). This indicates that substitutions towards a more stable PL occurred independently in the ophiuroid tree of life. Finally, we examined how these mutations impacted the global (rather than local) stability value of the protein. We found that 4 out of 5 mutations increased the global protein stability, including the site located in the substrate binding region (i.e. site 215 in the PL), confirming the results found with the local stability values.

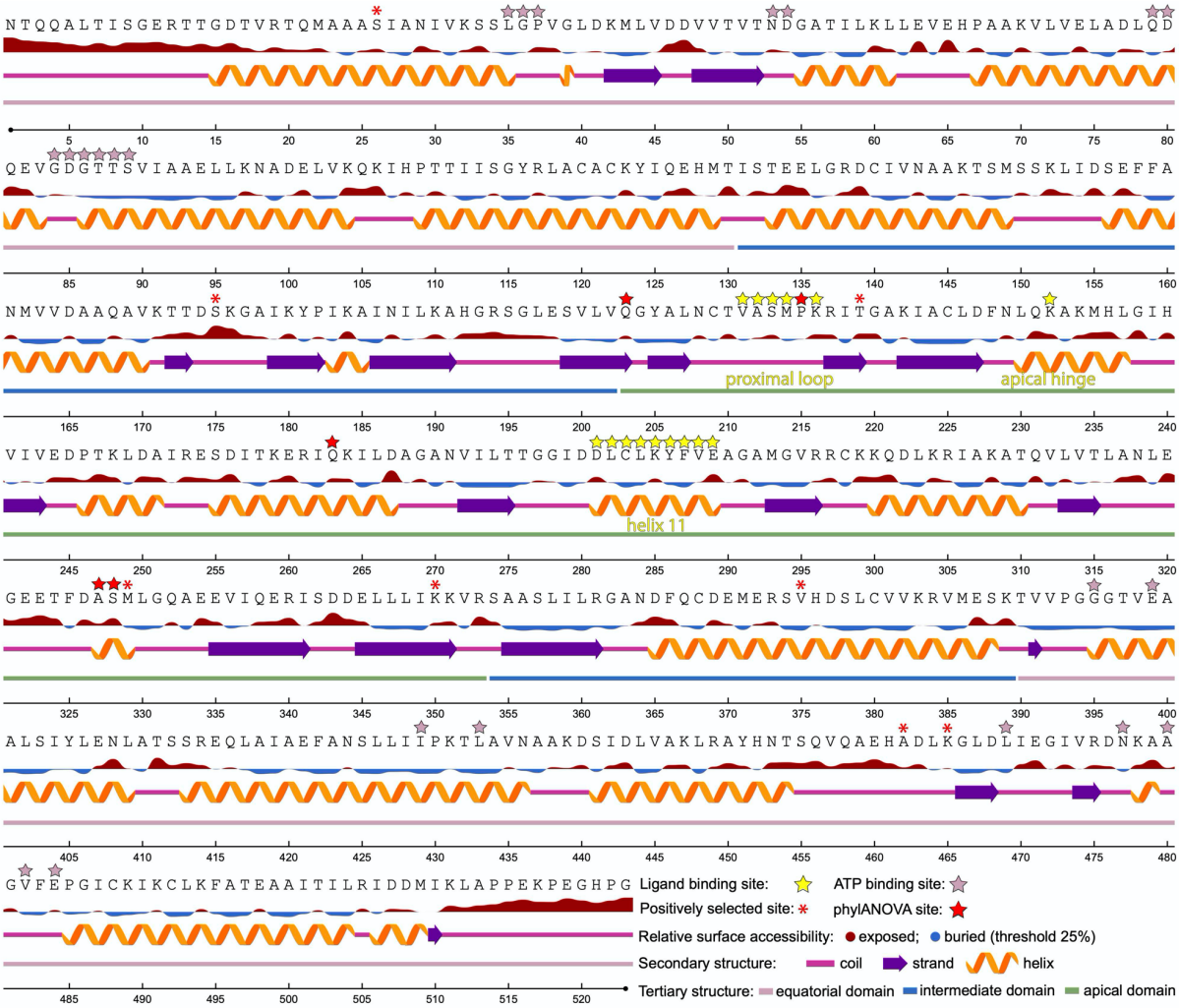

Fig. 3: Primary structure of CCTα. Ligand binding sites (proximal loop, apical hinge and helix 11), ATP binding sites, positively selected sites (method MEME) and sites displaying different local stability values between shallow and deep species (method phylANOVA) are highlighted. The sequence of the shallow-water Amphiuridae *Amphiura constricta* is used as template.

Discussion

Protein biogenesis is essential for deep-sea adaptation

In this study, we examined patterns of positive selection in 416 genes from four brittle star families representing replicated instances of deep-sea colonization. We found that four genes involved in functions related to protein biogenesis including protein folding and protein

375 synthesis (i.e. ribosomal proteins) were convergently positively selected in three out of four
376 families. Furthermore, an additional ribosomal protein was positively selected in
377 Ophiodermatidae and two transcription factors were positively selected in Amphiuridae.
378 Previous studies have shown that several genes involved in genetic information processing such
379 as protein folding, transcription or translation (including ribosomal proteins) were positively
380 selected in the hadal (>6000m depth) amphipod *Hirondella gigas* (Lan et al. 2017), in the
381 bathyal (200-3000m depth) fish *Aldrovandia affinis* (Lan et al. 2018) and in the bathyal barnacle
382 *Glyptelasma gigas* (Gan et al. 2020). Taken together, these and previous results indicate that
383 adaptations in protein biogenesis are essential to deep-sea life.

384 At the individual family level, four genes related to embryo development were positively
385 selected in Amphiuridae. Interestingly, nine genes related to the same function (embryo
386 development; GO: 0009790) were detected as candidate genes for deep-sea adaptation between
387 populations of the deep-sea fish *Coryphaenoides rupestris* living at different depths (Gaither et
388 al. 2018). This suggests that there might be similar selection pressures on development at both
389 young (i.e. species level) and old (i.e. family level) evolutionary timescales for life at great
390 depths. Finally, no candidate genes for deep-sea adaptation were found in Ophiotrichidae across
391 different positive selection methods. This might be explained by the fact that this family is the
392 youngest from a fossil and a phylogenetic point of view (O'Hara et al. 2017). In that sense, it
393 started colonizing the deep-sea later than the other families, and therefore there was possibly
394 less time for natural selection to act. In support with this, the maximum sampling depth for
395 Ophiotrichids was 405m, whereas it was deeper for the three other families (Amphiuridae:
396 5193m; Ophiodermatidae: 1668m; Ophiomyxidae: 792m).

397 *Independent evolutionary histories of subunits from macromolecular complexes*

398 CCTα and prefoldin 3 (PFD3), the two genes recurrently positively selected involved in protein
399 folding, are subunits of octameric and hexameric complexes, respectively. The CCT complex is
400 estimated to fold ~10% of newly synthesized proteins, including actin and tubulin, and is
401 involved in numerous core cellular processes such as cytoskeleton formation, cell signaling, cell
402 recognition and protein degradation (Bueno-Carrasco & Cuéllar 2019), while the prefoldin
403 complex is known to assist CCT in actin folding (Martín-Benito et al. 2002). We tested four
404 subunits of the octameric CCT complex, yet CCTα was the only one to show consistent
405 signatures of positive selection across different methods. Indeed, the other tested subunits
406 displayed relaxation of selection or no signatures of positive selection. This might be due to the
407 different degrees of subunit specialization in CCT, as CCTα has intermediate binding properties
408 (i.e. neither high ATP affinity nor high substrate affinity) compared to the other subunits
409 (Bueno-Carrasco & Cuéllar 2019). Therefore, it is possible that CCTα can evolve more rapidly
410 because it may experience less negative selection than the other subunits. In the same way, we
411 tested three subunits of the hexameric prefoldin complex, and PFD3 was the only subunit to be
412 consistently positively selected. While we acknowledge that we analyzed an existing dataset and
413 thus did not test all subunits of both macromolecular complexes (4/8 in CCT; 3/6 in prefoldin),
414 it appears surprising that individual subunits of macromolecular complexes can evolve
415 relatively independently from each other.

416 We note that a previous study actually highlighted evolutionary independence of CCT subunits
417 across old evolutionary timescales (i.e. among eukaryotes), showing that CCTα, CCTγ and CCTζ
418 evolved under positive selection after duplication events which led to sub-functionalization in

419 eukaryotes, most likely in response to folding increasingly complex cytosolic proteins (Fares &
420 Wolfe 2003). Furthermore, it has been shown that the exact same mutation in the conserved
421 ATP-binding region of all eight CCT subunits have dramatically different phenotypic outcomes
422 in yeast, such as differential temperature sensitivity, differential growth in presence of actin and
423 tubulin polymerization inhibitors, or differential over and under-expression of genes (Amit et al.
424 2010). This not only indicates that the functional activity of each subunit is not redundant but
425 also possibly highlights 'moonlighting' proteins (i.e. other functions of individual subunits that
426 are carried out not as part of the full complex) (Jeffery 2009; Huberts & van der Klei 2010). In
427 that sense, the functional coherence of several hetero-oligeromeric protein complexes including
428 CCT has been reviewed (Matalon et al. 2014). Interestingly, they found a lack of coherence
429 among subunits at virtually all functional levels, including different levels of subunit abundance,
430 differences in transcriptional regulation, differential subunit duplication or loss, and finally lack
431 of coherence in genetic interaction. Explanations for this lack of coherence include enhancing
432 complex assembly or subunit multi-functionality (Matalon et al. 2014). There is increasing
433 evidence for the latter case, as many CCT monomer functions have been reported and recently
434 reviewed (Vallin & Grantham 2019). Taken together, our results are consistent with the
435 hypothesis that CCTα and PFD3 may be moonlighting proteins involved in deep-sea adaptation.

436 *Convergent evolution, functional and structural adaptations in CCTα*

437 Our results suggest that convergent evolution was detected at the functional (i.e. protein
438 folding) and at the gene levels (i.e. CCTα, PFD3) in deep-sea adaptation. Yet, it was not detected
439 at the amino-acid level in CCTα, as the majority of positively selected sites were different among
440 families, except for one site shared between Amphiuridae and Ophiotrichidae. This might be due
441 to the old divergence time among the investigated brittle star families and the broad nature of
442 the selection regime (i.e. depth and temperature). It has been shown that rates of molecular
443 convergence decrease with time (Storz 2016) and the last common ancestor of Amphiuridae,
444 Ophiodermatidae and Ophiomyxidae is estimated to be approximately 250 million years old
445 (O'Hara et al. 2017). Furthermore, convergence at the amino-acid level is often less common
446 than convergence at higher levels of biological hierarchy (e.g. gene, pathway or species levels)
447 (Bolnick et al. 2018; Tenaillon et al. 2016, 2012).

448 Our results indicate that CCTα evolved under positive selection during deep-sea colonization
449 and speciation events. These mutations possibly reveal functional adaptations of CCTα, such as
450 adaptations in ATP or substrate binding. Indeed, it has previously been reported that the
451 shallow groove created by the conserved Helix 11 and the flexible Proximal Loop allows the
452 binding of a variety of substrates (Joachimiak et al. 2014; Yam et al. 2008), suggesting that the
453 detected substitutions in the PL and in adjacent amino acids allow efficient substrate binding in
454 deep-sea species. Similarly, in a study on metabolic enzymes from 37 ctenophores, numerous
455 sites associated with adaptation to depth, temperature or both were located close to the
456 substrate binding region (Winnikoff et al. 2019). A major substrate of the CCT complex and its
457 co-chaperone prefoldin is actin, an essential cytoskeleton protein (Martín-Benito et al. 2002).
458 While it should be noted that CCTα is not directly involved in actin folding (actin binds the
459 subunits CCTδ, CCTβ and CCTε) (Llorca et al. 1999, 2000), examination of cytoskeletal proteins
460 is of interest due to their essential role in cells. Unfortunately, as actin and tubulin were not
461 included in our dataset, no conclusions about cytoskeletal proteins of deep-sea brittle stars can
462 yet be drawn. However, actin of deep-sea fishes has been extensively studied, showing that it
463 displays structural adaptations to high-pressure enhancing stability (Morita 2003; Koyama &

464 Aizawa 2008; Wakai et al. 2014; Yancey 2020). Furthermore, genome analysis of the hadal fish
465 *Pseudoliparis swirei* revealed that a gene family related to cytoskeleton was expanded, and
466 several genes from three gene ontology categories linked to cytoskeleton were evolving under
467 positive selection (Wang et al. 2019). Finally, 13 genes involved in cytoskeleton systems were
468 positively selected in the deep-sea fish *A. affinis* (Lan et al. 2018), suggesting that cytoskeletal
469 proteins are pivotal for deep-sea adaptation.

470 Furthermore, we tested the hypothesis that CCTα is structurally adapted to deep-sea conditions,
471 as a common feature of high-pressure adapted proteins is to display increased stability (Somero
472 2003; Ohmae et al. 2013; Yancey & Siebenaller 2015). We investigated local and global stability
473 in CCTα and found that four out of five sites with phylogenetically-corrected significantly
474 different local stability showed increased global protein stability, suggesting that these
475 mutations reflect structural deep-sea adaptation. Moreover, seven out of eight mutations at
476 positively selected sites increased global protein stability, and involved hydrophobic amino-acid
477 substitutions, which are known to increase protein stability (Kellis et al. 1988; Pace et al. 2011).
478 It has also been shown that several proteins from the abyssal fish *Coryphaenoides armatus*
479 displayed increased protein stability as an adaptation to hydrostatic pressure (Morita 2003,
480 2008; Brindley et al. 2008; Lemaire et al. 2018). Finally, several critical mutations in both the
481 enzyme synthesizing trimethylamine oxide (TMAO: a heavily studied stabilizing cosolute or
482 piezolyte (Yancey 2020)) and in HSP90, have been proposed to enhance overall protein stability
483 in the hadal fish *Pseudoliparis swirei* (Wang et al. 2019).

484 *Role of molecular chaperones in deep-sea adaptation*

485 We have shown that over deep evolutionary timescales, CCTα displays recurrent signatures of
486 accelerated evolution and structural adaptation in transition from shallow to deep-sea habitats
487 in brittle stars. This contrasts with previous findings on sea urchins where, CCTε -but not the
488 other subunits- showed signatures of positive section, yet not in the two deep-sea species
489 included in the work (Kober & Pogson 2017). A functional equivalent of the eukaryotic
490 chaperonin CCT in bacteria is the chaperonin complex GroEL/GroES (Gupta 1990; Mayhew et al.
491 1996). This chaperonin has been shown to be constitutively highly expressed in the deep-sea
492 bacteria *Shewanella,* and that a major target of this chaperonin was a subunit of the 50S
493 ribosome (Sato et al. 2015). Furthermore, convergent evolution in chaperones has previously
494 been shown (Draceni & Pechmann 2019), and there is evidence that other groups of molecular
495 chaperones such as HSP70 and HSP90 (Kim et al. 2013) are involved in deep-sea adaptation
496 (Yancey 2020). For instance, the HSP70 gene family was expanded in a deep-sea mussel (Sun et
497 al. 2017) and convergent amino-acid changes have been reported in four out of five copies of the
498 HSP90 protein in a hadal fish (Wang et al. 2019). In our dataset, two HSP90 genes were present
499 (HSP90b1 and HSP90ab1), yet neither showed signatures of accelerated evolution.
500 Nevertheless, only the examination of whole genomes will give a complete view of HSP family
501 evolution in brittle stars, which should be explored in further studies.

502 *Similarities between deep-sea and cold adaptation mechanisms*

503 There are numerous studies on the role of CCT at shorter evolutionary timescales, which reveal
504 its role in cold-stress response. Notably, CCT has been characterized as a 'cold-shock' protein in
505 several eukaryotes due to the overexpression of the investigated subunits when organisms
506 were exposed to cold stress (He et al. 2017; Kayukawa et al. 2005; Somer et al. 2002; Yin et al.
507 2011). Furthermore, CCT has been shown to display specific structural (Pucciarelli et al. 2006)

508 and functional (Cuellar et al. 2014) adaptations to cold environment in Antarctic fish, in addition
509 to being also overexpressed in Antarctic fish exposed to heat stress (Buckley & Somero 2009).
510 Moreover, there is evidence for a link between cold-stress response and high-pressure stress
511 response in bacteria (Welch et al. 1993; Wemekamp-Kamphuis et al. 2002), although it has also
512 been shown that heat-shock proteins are also expressed under high-pressure stress in bacteria
513 (Aertsen et al. 2004) or constitutively in the deep-sea bacteria *Shewanella* (Sato et al. 2015).
514 Additionally, transcriptome analyses revealed that cold-inducible protein families are expanded
515 in a hadal amphipod (Lan et al. 2017), and several proteins involved in cold shock have been
516 shown to evolve under positive selection in deep-sea amphipod and fish (Lan et al. 2018). Taken
517 together, our findings support the hypothesis that cold shock proteins play an important role in
518 deep-sea adaptation (Brown & Thatje 2014), which was also proposed by others (Lan et al.
519 2018).

520 *Limitations and outlook*

521 We acknowledge that our study lacks functional validation to demonstrate that the changes are
522 truly adaptive (which would be experimentally demanding as CCT folds ~10% of newly
523 synthesized proteins and we analyzed the sequences of more than 700 species), yet we
524 minimized false inferences by applying stringent positive selection detection criteria.
525 Furthermore, we used a *proxy* of functional validation by investigating *in silico* local and global
526 protein stability in a dataset with great comparative power, both in terms of phylogenetic and
527 environmental diversity. Finally, direct experimental testing on deep-sea organisms remains
528 technically challenging, so we made use of the power of molecular data to indirectly reveal new
529 insights in deep-sea adaptation. Further studies should include whole genomes to obtain a more
530 complete view of deep-sea adaptation hotspots and possible mechanisms, such as recent studies
531 on deep-sea fishes (Gaither et al. 2018; Wang et al. 2019), hydrothermal vent mussel (Sun et al.
532 2017) or cold seep gastropod (Liu et al. 2020). Also, while we focused on intrinsic adaptations
533 (i.e. at the genomic level), mechanisms of extrinsic adaptations (i.e. changes in the cellular
534 milieu) through, for instance, osmolyte concentration (piezolytes such as TMAO) or membrane
535 phospholipid composition changes, should not be overlooked (Yancey & Siebenaller 2015;
536 Somero 2003; Yancey 2020). However, this is beyond the scope of this study. With increasing
537 interests in deep-sea biodiversity, ecosystems and resources in the last decades (Danovaro et al.
538 2017, 2014; Glover et al. 2018), these are exciting times for diving deeper into mechanisms of
539 deep-sea adaptation.

540 **References**

541 Aertsen A et al. 2004. Heat shock protein-mediated resistance to high hydrostatic pressure in *Escherichia*
542 *coli.* Appl Env. Microbiol. 70:2660–2666.

543 Amit M et al. 2010. Equivalent mutations in the eight subunits of the chaperonin CCT produce
544 dramatically different cellular and gene expression phenotypes. J. Mol. Biol. 401:532–543.

545 Bolnick DI, Barrett RD, Oke KB, Rennison DJ, Stuart YE. 2018. (Non) parallel evolution. Annu. Rev. Ecol.
546 Evol. Syst. 49:303–330.

547 Bribiesca-Contreras G, Verbruggen H, Hugall AF, O'Hara TD. 2017. The importance of offshore origination
548 revealed through ophiuroid phylogenomics. In: Proc. R. Soc. B.Vol. 284 The Royal Society p. 20170160.

549 Brindley AA et al. 2008. Enzyme sequence and its relationship to hyperbaric stability of artificial and
550 natural fish lactate dehydrogenases. PLoS One. 3.

551 Brown A, Thatje S. 2014. Explaining bathymetric diversity patterns in marine benthic invertebrates and
552 demersal fishes: physiological contributions to adaptation of life at depth. Biol. Rev. 89:406–426.

553 Buckley BA, Somero GN. 2009. cDNA microarray analysis reveals the capacity of the cold-adapted
554 Antarctic fish *Trematomus bernacchii* to alter gene expression in response to heat stress. Polar Biol.
555 32:403–415.

556 Bueno-Carrasco MT, Cuéllar J. 2019. Mechanism and Function of the Eukaryotic Chaperonin CCT. ELS John
557 Wiley Sons Ltd Ed. 1–9. doi: 10.1002/9780470015902.a0028208.

558 Carney RS. 2005. Zonation of deep biota on continental margins. In: Oceanography and Marine Biology.
559 CRC Press pp. 221–288.

560 Christodoulou M, O'Hara Timothy, et al. 2019a. Unexpected high abyssal ophiuroid diversity in
561 polymetallic nodule fields of the Northeast Pacific Ocean, and implications for conservation.
562 Biogeosciences Discuss. 1–54.

563 Christodoulou M, O'Hara Timothy D., Hugall AF, Arbizu PM. 2019b. Dark Ophiuroid Biodiversity in a
564 Prospective Abyssal Mine Field. Curr. Biol. 29:3909–3912.

565 Conesa A et al. 2005. Blast2GO: a universal tool for annotation, visualization and analysis in functional
566 genomics research. Bioinformatics. 21:3674–3676. doi: 10.1093/bioinformatics/bti610.

567 Cuellar J et al. 2014. Assisted protein folding at low temperature: evolutionary adaptation of the Antarctic
568 fish chaperonin CCT and its client proteins. Biol. Open. 3:261–270.

569 Dahlhoff E, Somero GN. 1991. Pressure and temperature adaptation of cytosolic malate dehydrogenases
570 of shallow and deep-living marine invertebrates: evidence for high body temperatures in hydrothermal
571 vent animals. J. Exp. Biol. 159:473–487.

572 Danovaro R, Corinaldesi C, Dell'Anno A, Snelgrove PV. 2017. The deep-sea under global change. Curr. Biol.
573 27:R461–R465.

574 Danovaro R, Snelgrove PV, Tyler P. 2014. Challenging the paradigms of deep-sea ecology. Trends Ecol.
575 Evol. 29:465–475.

576 D'Aquino JA et al. 1996. The magnitude of the backbone conformational entropy change in protein
577 folding. Proteins Struct. Funct. Bioinforma. 25:143–156.

578 Draceni Y, Pechmann S. 2019. Pervasive convergent evolution and extreme phenotypes define chaperone
579 requirements of protein homeostasis. Proc. Natl. Acad. Sci. 116:20009–20014.

580 Fares MA, Wolfe KH. 2003. Positive selection and subfunctionalization of duplicated CCT chaperonin
581 subunits. Mol. Biol. Evol. 20:1588–1597.

582 Fields PA, Dong Y, Meng X, Somero GN. 2015. Adaptations of protein structure and function to
583 temperature: there is more than one way to 'skin a cat'. J. Exp. Biol. 218:1801–1811.

584 Gaither MR et al. 2016. Depth as a driver of evolution in the deep sea: Insights from grenadiers
585 (Gadiformes: Macrouridae) of the genus Coryphaenoides. Mol. Phylogenet. Evol. 104:73–82. doi:
586 10.1016/j.ympev.2016.07.027.

587 Gaither MR et al. 2018. Genomics of habitat choice and adaptive evolution in a deep-sea fish. Nat. Ecol.
588 Evol. 2:680.

589 Gan Z et al. 2020. Comparative transcriptomic analysis of deep-and shallow-water barnacle species
590 (Cirripedia, Poecilasmatidae) provides insights into deep-sea adaptation of sessile crustaceans. BMC
591 Genomics. 21:1–13.

592 Gestaut D et al. 2019. The Chaperonin TRiC/CCT Associates with Prefoldin through a Conserved
593 Electrostatic Interface Essential for Cellular Proteostasis. Cell. 177:751–765.

594 Glover AG, Wiklund H, Chen C, Dahlgren TG. 2018. Point of View: Managing a sustainable deep-sea 'blue
595 economy'requires knowledge of what actually lives there. eLife. 7:e41319.

596 Gross M, Jaenicke R. 1994. Proteins under pressure: the influence of high hydrostatic pressure on
597 structure, function and assembly of proteins and protein complexes. Eur. J. Biochem. 221:617–630.

598 Gu J, Hilser VJ. 2008. Predicting the energetics of conformational fluctuations in proteins from sequence: a
599 strategy for profiling the proteome. Structure. 16:1627–1637.

600 Gu J, Hilser VJ. 2009. Sequence-based analysis of protein energy landscapes reveals nonuniform thermal
601 adaptation within the proteome. Mol. Biol. Evol. 26:2217–2227.

602 Gupta RS. 1990. Sequence and structural homology between a mouse T-complex protein TCP-1 and
603 the'chaperonin'family of bacterial (GroEL, 60-65 kDa heat shock antigen) and eukaryotic proteins.
604 Biochem. Int. 20:833–841.

605 He Y, Wang L, Zhu W, Dong Z, Liu N. 2017. Effects of salinity on cold tolerance of Malaysian red tilapia.
606 Aquac. Int. 25:777–792.

607 Holm S. 1979. A simple sequentially rejective multiple test procedure. Scand. J. Stat. 65–70.

608 Huberts DHEW, van der Klei IJ. 2010. Moonlighting proteins: An intriguing mode of multitasking. Biochim.
609 Biophys. Acta BBA - Mol. Cell Res. 1803:520–525. doi: 10.1016/j.bbamcr.2010.01.022.

610 Hugall AF, O'Hara TD, Hunjan S, Nilsen R, Moussalli A. 2015. An exon-capture system for the entire class
611 Ophiuroidea. Mol. Biol. Evol. 33:281–294.

612 Jaenicke R. 1991. Protein stability and molecular adaptation to extreme conditions. In: EJB Reviews 1991.
613 Springer pp. 291–304.

614 Jeffery CJ. 2009. Moonlighting proteins—an update. Mol. Biosyst. 5:345–350.

615 Joachimiak LA, Walzthoeni T, Liu CW, Aebersold R, Frydman J. 2014. The structural basis of substrate
616 recognition by the eukaryotic chaperonin TRiC/CCT. Cell. 159:1042–1055.

617 Kayukawa T et al. 2005. Expression of mRNA for the t; chcomplex polypeptide–1, a subunit of chaperonin
618 CCT, is upregulated in association with increased cold hardiness in *Delia antiqua*. Cell Stress Chaperones.
619 10:204.

620 Kelley LA, Mezulis S, Yates CM, Wass MN, Sternberg MJ. 2015. The Phyre2 web portal for protein
621 modeling, prediction and analysis. Nat. Protoc. 10:845.

622 Kellis JT, Nyberg K, S˘ail D, Fersht AR. 1988. Contribution of hydrophobic interactions to protein stability.
623 Nature. 333:784–786. doi: 10.1038/333784a0.

624 Khan S, Vihinen M. 2010. Performance of protein stability predictors. Hum. Mutat. 31:675–684.

625 Khatun J, Khare SD, Dokholyan NV. 2004. Can contact potentials reliably predict stability of proteins? J.
626 Mol. Biol. 336:1223–1238.

627 Kim YE, Hipp MS, Bracher A, Hayer-Hartl M, Ulrich Hartl F. 2013. Molecular chaperone functions in
628 protein folding and proteostasis. Annu. Rev. Biochem. 82:323–355.

629 Kober KM, Pogson GH. 2017. Genome-wide signals of positive selection in strongylocentrotid sea urchins.
630 BMC Genomics. 18:555.

631 Koyama S, Aizawa M. 2008. Piezotolerance of the cytoskeletal structure in cultured deep-sea fish cells
632 using DNA transfection and protein introduction techniques. Cytotechnology. 56:19–26.

633 Lan Y et al. 2018. De novo transcriptome assembly and positive selection analysis of an individual deep-
634 sea fish. BMC Genomics. 19:394.

635 Lan Y et al. 2017. Molecular adaptation in the world's deepest-living animal: Insights from transcriptome
636 sequencing of the hadal amphipod *Hirondellea gigas*. Mol. Ecol. 26:3732–3743.

637 Lemaire B et al. 2018. Molecular adaptation to high pressure in cytochrome P450 1A and aryl
638 hydrocarbon receptor systems of the deep-sea fish *Coryphaenoides armatus*. Biochim. Biophys. Acta BBA-
639 Proteins Proteomics. 1866:155–165.

640 Liu R et al. 2020. De novo genome assembly of limpet *Bathyacmaea lactea* (Gastropoda: Pectinodontidae),
641 the first reference genome of a deep-sea gastropod endemic to cold seeps. Genome Biol. Evol. doi:
642 10.1093/gbe/evaa100.

643 Llorca O et al. 2000. Eukaryotic chaperonin CCT stabilizes actin and tubulin folding intermediates in open
644 quasi-native conformations. EMBO J. 19:5971–5979.

645 Llorca O et al. 1999. Eukaryotic type II chaperonin CCT interacts with actin through specific subunits.
646 Nature. 402:693–696.

647 Martín-Benito J et al. 2002. Structure of eukaryotic prefoldin and of its complexes with unfolded actin and
648 the cytosolic chaperonin CCT. EMBO J. 21:6377–6386.

649 Matalon O, Horovitz A, Levy ED. 2014. Different subunits belonging to the same protein complex often
650 exhibit discordant expression levels and evolutionary properties. Curr. Opin. Struct. Biol. 26:113–120.

651 Mayhew M et al. 1996. Protein folding in the central cavity of the GroEL–GroES chaperonin complex.
652 Nature. 379:420–426.

653 Morita T. 2008. Comparative sequence analysis of myosin heavy chain proteins from congeneric shallow-
654 and deep-living rattail fish (genus *Coryphaenoides*). J. Exp. Biol. 211:1362–1367.

655 Morita T. 2003. Structure-based analysis of high pressure adaptation of α-actin. J. Biol. Chem. 278:28060–
656 28066.

657 Murrell B et al. 2012. Detecting individual sites subject to episodic diversifying selection. PLoS Genet.
658 8:e1002764.

659 Murrell B et al. 2015. Gene-wide identification of episodic selection. Mol. Biol. Evol. 32:1365–1371.

660 O'Hara TD, Hugall AF, Thuy B, Moussalli A. 2014. Phylogenomic resolution of the class Ophiuroidea
661 unlocks a global microfossil record. Curr. Biol. 24:1874–1879.

662 O'Hara TD, Hugall AF, Thuy B, Stöhr S, Martynov AV. 2017. Restructuring higher taxonomy using broad-
663 scale phylogenomics: The living Ophiuroidea. Mol. Phylogenet. Evol. 107:415–430.

664 O'Hara TD, Hugall AF, Woolley SN, Bribiesca-Contreras G, Bax NJ. 2019. Contrasting processes drive
665 ophiuroid phylodiversity across shallow and deep seafloors. Nature. 565:636.

666 Ohmae E, Miyashita Y, Kato C. 2013. Thermodynamic and functional characteristics of deep-sea enzymes
667 revealed by pressure effects. Extremophiles. 17:701–709. doi: 10.1007/s00792-013-0556-2.

668 Oliver TA et al. 2010. Whole-genome positive selection and habitat-driven evolution in a shallow and a
669 deep-sea urchin. Genome Biol. Evol. 2:800–814.

670 Pace CN et al. 2011. Contribution of Hydrophobic Interactions to Protein Stability. J. Mol. Biol. 408:514–
671 528. doi: 10.1016/j.jmb.2011.02.053.

672 Pradillon F, Gaill F. 2007. Adaptation to deep-sea hydrothermal vents: some molecular and developmental
673 aspects. J. Mar. Sci. Technol. 37–53.

674 Pucciarelli S, Parker SK, Detrich HW, Melki R. 2006. Characterization of the cytoplasmic chaperonin
675 containing TCP-1 from the Antarctic fish *Notothenia coriiceps*. Extremophiles. 10:537–549.

676 Ramirez-Llodra EZ et al. 2010. Deep, diverse and definitely different: unique attributes of the world's
677 largest ecosystem. Biogeosciences. 7:2851–2899. doi: 10.5194/bg-7-2851-2010.

678 Rey C, Guéguen L, Sémon M, Boussau B. 2018. Accurate detection of convergent amino-acid evolution
679 with PCOC. Mol. Biol. Evol. 35:2296–2306.

680 Reynolds CR, Islam SA, Sternberg MJ. 2018. EzMol: A web server wizard for the rapid visualization and
681 image production of protein and nucleic acid structures. J. Mol. Biol. 430:2244–2248.

682 Saarman NP, Kober KM, Simison WB, Pogson GH. 2017. Sequence-based analysis of thermal adaptation
683 and protein energy landscapes in an invasive blue mussel (*Mytilus galloprovincialis*). Genome Biol. Evol.
684 9:2739–2751.

685 Sato H, Nakasone K, Yoshida T, Kato C, Maruyama T. 2015. Increases of heat shock proteins and their
686 mRNAs at high hydrostatic pressure in a deep-sea piezophilic bacterium, *Shewanella violacea*.
687 Extremophiles. 19:751–762.

688 Schymkowitz J et al. 2005. The FoldX web server: an online force field. Nucleic Acids Res. 33:W382–
689 W388.

690 Siebenaller J, Somero GN. 1978. Pressure-adaptive differences in lactate dehydrogenases of congeneric
691 fishes living at different depths. Science. 201:255–257.

692 Siebenaller JF. 2010. Effects of the deep-sea environment on invertebrates. Comp. High Press. Biol. 319–
693 341.

694 Siebenaller JF, Somero GN. 1979. Pressure-adaptive differences in the binding and catalytic properties of
695 muscle-type (M 4) lactate dehydrogenases of shallow-and deep-living marine fishes. J. Comp. Physiol.
696 129:295–300.

697 Smith MD et al. 2015. Less is more: an adaptive branch-site random effects model for efficient detection of
698 episodic diversifying selection. Mol. Biol. Evol. 32:1342–1353.

699 Somer L, Shmulman O, Dror T, Hashmueli S, Kashi Y. 2002. The eukaryote chaperonin CCT is a cold shock
700 protein in *Saccharomyces cerevisiae*. Cell Stress Chaperones. 7:47.

701 Somero GN. 1992. Adaptations to high hydrostatic pressure. Annu. Rev. Physiol. 54:557–577.

702 Somero GN. 1990. Life at low volume change: hydrostatic pressure as a selective factor in the aquatic
703 environment. Am. Zool. 30:123–135.

704 Somero GN. 2003. Protein adaptations to temperature and pressure: complementary roles of adaptive
705 changes in amino acid sequence and internal milieu. Comp. Biochem. Physiol. B Biochem. Mol. Biol.
706 136:577–591. doi: 10.1016/S1096-4959(03)00215-X.

707 Stöhr S, O'Hara TD, Thuy B. 2012. Global diversity of brittle stars (Echinodermata: Ophiuroidea). PLoS
708 ONE. 7:e31940. doi: 10.1371/journal.pone.0031940.

709 Stöhr S, O'Hara TD, Thuy B. 2017. World Ophiuroidea Database. Accessed at
710 http://www.marinespecies.org/ophiuroidea on 2017-07-27.

711 Storz JF. 2016. Causes of molecular convergence and parallelism in protein evolution. Nat. Rev. Genet.
712 17:239–250.

713 Suka A et al. 2019. Stability of cytochromes c′ from psychrophilic and piezophilic *Shewanella* species:
714 implications for complex multiple adaptation to low temperature and high hydrostatic pressure.
715 Extremophiles. 23:239–248.

716 Sun J et al. 2017. Adaptation to deep-sea chemosynthetic environments as revealed by mussel genomes.
717 Nat. Ecol. Evol. 1:0121.

718 Tenaillon O et al. 2016. Tempo and mode of genome evolution in a 50,000-generation experiment. Nature.
719 536:165.

720 Tenaillon O et al. 2012. The molecular diversity of adaptive convergence. Science. 335:457–461.

721 Vallin J, Grantham J. 2019. The role of the molecular chaperone CCT in protein folding and mediation of
722 cytoskeleton-associated processes: implications for cancer cell biology. Cell Stress Chaperones. 24:17–27.

723 Valpuesta JM, Carrascosa JL, Willison KR. 2005. Structure and function of the cytosolic chaperonin CCT.
724 Protein Fold. Handb. 725–755.

725 Venkat A, Hahn MW, Thornton JW. 2018. Multinucleotide mutations cause false inferences of lineage-
726 specific positive selection. Nat. Ecol. Evol. 2:1280.

727 Wakai N, Takemura K, Morita T, Kitao A. 2014. Mechanism of deep-sea fish α-actin pressure tolerance
728 investigated by molecular dynamics simulations. PloS One. 9:e85852.

729 Wang K et al. 2019. Morphology and genome of a snailfish from the Mariana Trench provide insights into
730 deep-sea adaptation. Nat. Ecol. Evol. 3:823–833.

731 Weber AA-T et al. 2017. Positive selection on sperm ion channels in a brooding brittle star: consequence
732 of life-history traits evolution. Mol. Ecol. 26:3744–3759.

733 Welch TJ, Farewell A, Neidhardt FC, Bartlett DH. 1993. Stress response of *Escherichia coli* to elevated
734 hydrostatic pressure. J. Bacteriol. 175:7170–7177.

735 Wemekamp-Kamphuis HH, Karatzas AK, Wouters JA, Abee T. 2002. Enhanced levels of cold shock
736 proteins in *Listeria monocytogenes* LO28 upon exposure to low temperature and high hydrostatic
737 pressure. Appl Env. Microbiol. 68:456–463.

738 Wertheim JO, Murrell B, Smith MD, Kosakovsky Pond SL, Scheffler K. 2014. RELAX: detecting relaxed
739 selection in a phylogenetic framework. Mol. Biol. Evol. 32:820–832.

740 Winnikoff JR, Francis WR, Thuesen EV, Haddock SHD. 2019. Combing transcriptomes for secrets of deep-
741 sea survival: Environmental diversity drives patterns of protein evolution. Integr. Comp. Biol.

742 Woolley SN et al. 2016. Deep-sea diversity patterns are shaped by energy availability. Nature. 533:393–
743 410.

744 Yam AY et al. 2008. Defining the TRiC/CCT interactome links chaperonin function to stabilization of newly
745 made proteins with complex topologies. Nat. Struct. Mol. Biol. 15:1255.

746 Yancey PH. 2020. Cellular responses in marine animals to hydrostatic pressure. J. Exp. Zool. Part Ecol.
747 Integr. Physiol. early online version. doi: 10.1002/jez.2354.

748 Yancey PH, Siebenaller JF. 2015. Co-evolution of proteins and solutions: protein adaptation versus
749 cytoprotective micromolecules and their roles in marine organisms. J. Exp. Biol. 218:1880–1896.

750 Yin Q et al. 2011. Molecular cloning of Litopenaeus vannamei TCP-1-eta gene and analysis on its
751 relationship with cold tolerance. Yi Chuan Hered. 33:168–174.

752 Zhang Yanjie et al. 2017. Adaptation and evolution of deep-sea scale worms (Annelida: Polynoidae):
753 insights from transcriptome comparison with a shallow-water species. Sci. Rep. 7:46205.

754

755 **Acknowledgements**

756 We are grateful to W. Salzburger for providing access to the HPC sciCORE cluster and to J.
757 Sarrazin and S. Arnaud-Haond for comments on a previous version of this manuscript. We thank
758 L. Bribiesca-Contreras for help with R analyses. We thank three anonymous reviewers and the
759 editorial team for valuable comments on a previous version of this manuscript. Calculations
760 were performed at sciCORE (http://scicore.unibas.ch/) scientific computing center at the
761 University of Basel, Switzerland and at DATARMOR (http://www.ifremer.fr/pcdm) scientific

computing center at the Pôle de Calcul et de Données Marines (PCDM), Ifremer, Brest, France. This work was supported by an Endeavour Postdoctoral Fellowship awarded by the Australian Department of Education and Training [grant number 6534_2018 to AATW] and a Marie Sklodowska-Curie Global Fellowship awarded by the European Union's Horizon 2020 research and innovation programme [grant number 797326 to AATW].

Data deposition

Phylogenomic data (including raw reads) and scripts for dataset generation are available in NCBI Bioproject PRJNA311384 and dryad packages: https://doi.org/10.5061/dryad.db339/10 and https://datadryad.org/stash/dataset/doi:10.5061/dryad.rb334.

Conflict of interest

None

Supplementary figure captions

Fig. S1: Overlap of positively selected candidate genes among three brittle star families. A: Number of candidate genes per family positively selected in at least three positive selection detection methods and not displaying relaxation of selection. B: Number of candidate genes per family positively selected in all four positive selection detection methods and not displaying relaxation of selection. In both conditions of A and B, no gene was positively selected in the family Ophiotrichidae.

Fig. S2: Maximum-likelihood reconstruction of CCTα using amino-acid sequences. The four focal families (Amphiuridae, Ophiotrichae, Ophiomyxidae and Ophiodermatidae) and the outgroup (Asteronychidae) are labelled. Positively selected lineages (aBSREL method) of each family are highlighted in red.

Fig. S3: Comparison of local stability values from CCTα apical domain between shallow and deep species. A: Log transformed p-values of the phylogenetically-corrected ANOVA performed between average delta G values of shallow vs. deep species at each codon of the CCTα apical domain. The substrate binding regions PL, AH and H11 are highlighted in light orange. The positively selected sites are highlighted with a red star. P-value level corresponding to 0.05 is highlighted in red. The most significant codons in a "significance peak" (204, 214, 265 and 324) are highlighted. B: Beanplots of delta G values between shallow (0-200m) and deep (>200m) species for each one of the most significant codons in the phylogenetically-corrected ANOVA. Horizontal bar represents the average value of the dataset.

Fig. S4: Comparison of local stability values over 10-codon windows on the complete CCTα gene between shallow and deep species. A: Average protein stability profiles over 10 codon windows for the complete CCTα gene in 324 species (424 individuals) from shallow water (0-200m) and 401 species (543 individuals) from deep water (>200m) representative of the whole ophiuroid class. A smaller (i.e. more negative) value of delta G is indicative of substitutions increasing stability. The positively selected sites are highlighted with a red star. B: Log transformed p-values of the phylogenetically-corrected ANOVA performed between average delta G values over 10 codon windows of shallow vs. deep species. The positively selected sites are highlighted with a red star. P-value level corresponding to 0.05 is highlighted in red. C: Beanplots of delta G values between shallow (0-200m) and deep (>200m) species for both of the most significant 10 codon windows in the phylogenetically-corrected ANOVA. Horizontal bar represents the average value of the dataset.

Supplementary tables (in separate excel file)

Table S1: List of species used in this study, GPS coordinates and environmental parameters at their sampling locations. Empty cells indicate missing data.

804 **Table S2:** Positively selected candidate genes per family and their Gene Ontology annotation (P:
805 Biological Process; F: Molecular Function; C: Cellular Component). Genes positively selected in several
806 families are highlighted in bold.

807 **Table S3:** Results of positive selection tests in shallow-water lineages for the five candidate genes for
808 deep-sea adaptation. Significance level: 0.05. Significant results are in bold. NS: not significant

809 **Table S4:** Results of positive selection tests for the three prefoldin subunits for each family. Significance
810 level: 0.05. Significant results are in bold. NS: not significant

811 **Table S5:** Sites displaying episodic positive selection in CCTα. Method used: MEME. Significance level:
812 0.05. Significant sites are in bold.

813 **Table S6:** Results of positive selection tests for the four CCT subunits for each family. Significant results
814 are in bold. Significance level: 0.05. NS: not significant